Combust. Sci. and Tech., 181: 433–456, 2009

ISSN: 0010-2202 print/1563-521X online
DOI: 10.1080/00102200802612351

Taylor & Francis
Taylor & Francis Group

PREDICTION AND MEASUREMENT OF THE PRODUCT GAS COMPOSITION OF THE ULTRA RICH PREMIXED COMBUSTION OF NATURAL GAS: EFFECTS OF EQUIVALENCE RATIO, RESIDENCE TIME, PRESSURE, AND OXYGEN CONCENTRATION

Bogdan A. Albrecht, Jim B. W. Kok, Nutte Dijkstra, and Theo van der Meer
University of Twente, The Netherlands

The ultra rich combustion (partial oxidation) of natural gas to hydrogen and carbon monoxide is theoretically and experimentally investigated. The effect of the process parameters equivalence ratio, residence time, pressure, and composition of the oxidizer is explored. Computations are performed with the use of the chemical kinetics simulation package CHEMKIN. First, the ultra rich combustion process is modeled as a freely propagating flame in order to establish the rich flame propagation properties. An Arrhenius correlation of the laminar flame speed with the adiabatic flame temperature is found with activation temperature 20,000 K. Subsequently, perfectly stirred reactor (PSR) computations were performed. From these, it is concluded that optimal natural gas conversion to hydrogen and carbon monoxide requires a residence time of at least 50 ms and, depending on residence time, an equivalence ratio between 2 and 4. To reach chemical equilibrium in ultra rich mixtures, the residence time is very long (>1000 ms). The model predictions are validated by experiments on ultra rich combustion of natural gas by means of air enriched to 40% oxygen concentration at up to 3 bar and 300 kW. The effect of equivalence ratio at residence time 50 ms was investigated. Good comparison was found between measurements and model predictions on carbon monoxide, hydrogen, and the soot precursor acetylene. It can be concluded that the model provides reliable information on product gas concentrations as a result of ultra rich combustion of natural gas.

Keywords: Gasification; Hydrogen; Natural gas; Rich combustion; Soot; Syngas

INTRODUCTION

Ultra rich combustion (gasification) of hydrocarbons is a process applied to produce synthesis gas (or syngas). This gas is composed primarily of hydrogen and carbon monoxide. Syngas represents the intermediary step from hydrocarbons to bulk chemicals (for example, acetic acid, methanol, DME, oxo-alcohols,

Received 31 March 2008; revised 19 October 2008; accepted 23 October 2008.

Bogdan A. Albrecht is presently at Advanced Engineering Engines, DAF Trucks N.V., Hugo van der Goeslaan 1, P.O. Box 90065, 5600 PT Eindhoven, The Netherlands.

This research project was supported by PiT, the Twente Research School for Process Technology and Senter, an Agency of the Dutch Ministry of Economic Affairs, grant EDI 01015.

Address correspondence to Jim B. W. Kok, University of Twente, P.O. Box 217, 7500 AE Enschede, The Netherlands. E-mail: j.b.w.kok@utwente.nl

isocyanates, ammonia) and synthetic fuels (synthetic diesel) (Christensen & Primdahl, 1994). The ultra rich combustion of methane can be described by the following global reaction:

$$CH_4 + 0.5O_2 = CO + 2H_2,\ \Delta h = -36\,\mathrm{KJ\,mol^{-1}}. \quad (1)$$

In Eq. (1), the negative value of the heat of reaction Δh indicates that the rich combustion process is exothermic when viewed from reactants to products.. In industrial applications of this process, temperatures range between 1400 and 1800 K and pressures are up to 150 bar (Albrecht, 2004; Albrecht et al., 2007). Due to the high temperature and pressure of the syngas produced by ultra rich combustion, the syngas sensible heat can be efficiently converted to power by expansion in a gas turbine expander (Albrecht, 2004; Albrecht et al., 2007). To analyze the performance of the reactor with a view to bulk chemicals production, the composition of the syngas can be estimated at equilibrium. This estimate, however, is very inaccurate, as in practical reactor designs, the syngas is produced in conditions far from chemical equilibrium. For this reason, the non-chemical equilibrium performance of the ultra rich combustion reactor, taking chemical kinetic effects into account, is important. The reactor design and the operating conditions have to ensure a high conversion of natural gas to products (i.e., hydrogen and carbon monoxide). In addition to this, the hydrogen to carbon monoxide ratio in the syngas is relevant for the downstream application of the syngas produced. For example, a syngas suitable for synthetic fuel production by the Fisher-Tropsch process has a hydrogen to carbon monoxide molar ratio of 2 (Van de Burght & Van Leeuwen, 1988). Finally the syngas soot content is of concern, in view of the syngas fouling the reactor system and to minimize the downstream effort of soot removal. For these reasons, the rich combustion process inside the reactor is investigated in the present paper, taking into account chemical kinetics in two characteristic types of reactors. In doing that, simplified models for the ultra rich combustion reactor are applied and CHEMKIN-II codes are used.

In the ultra rich combustion process, natural gas is converted to syngas with the use of an oxidizer. The oxidizer composition depends on the subsequent utilization of the syngas. When nitrogen is not desired in the syngas (e.g., for the production of synthetic diesel or methanol), the oxidizer is pure oxygen. When syngas is used for the production of ammonia, the oxidizer is air or oxygen enriched air. The natural gas can have different compositions as well, depending on its origin. Therefore, two types of mixtures were considered for the present investigation. One of them consists of pure methane (CH_4) and pure oxygen (O_2), and the other consists of natural gas and oxygen enriched air. The natural gas (NG) composition is taken as 85% vol. CH_4 and 15% vol. N_2. This composition was chosen to give the lower heating value of the Dutch natural gas produced by the Groningen reservoir (Geerssen, 1988). The oxygen enriched air (hereafter abbreviated as NITROX) is composed of 40% vol. O_2 and 60% vol. N_2.

In this article, the results of simulations of the ultra rich combustion process in a freely propagating flame are presented. The freely propagating flame configuration gives information about the propagation properties of rich flames, as encountered in the ultra rich combustion process. We also discuss results of simulations of the ultra rich combustion process in a perfectly stirred reactor (PSR). The PSR configuration

Table 1 Optimization conditions for the reaction mechanism GRI-Mech 3.0

Parameter	Value
Temperature (K)	1000–2500
Pressure (Pa)	150–10^6
Fuel equivalence ratio	0.1–5

is characterized by perfect mixing between reactants and products in a reactor volume with finite size and residence time. This case shows the limits of improving natural gas conversion by enhancing the mixing inside the ultra rich combustion reactor. The analyzed parameters are residence time, equivalence ratio, pressure, and oxidizer composition. The effect of the variation of these process parameters on the syngas composition, temperature, and flame speed is also investigated.

The simulations have been performed with the CHEMKIN-II chemical kinetics simulation codes PREMIX, PSR, and EQUIL (Kee et al., 1989). The chemistry is described by the detailed reaction mechanism GRI-Mech 3.0, developed by Bowman et al. (2001; see also Smith et al., 2000). It consists of 325 reactions and 53 species, and it was optimized for the conditions presented in Table 1. It can be noticed that the rich mixtures that correspond to ultra rich combustion processes (equivalence ratio of 3–4) fall within the equivalence ratio range for which the mechanism GRI-Mech 3.0 was optimized. The choice of GRI-Mech 3.0 for simulating the combustion of rich mixtures is supported by results obtained with this mechanism by other investigators (Musick et al., 1996). In Musick et al. (1996), laminar $CH_4/O_2/Ar$ flames at equivalence ratios between 0.92 and 1.94 and low pressure (20–60 Torr) have been simulated using the PREMIX code. Eight reaction mechanisms have been tested, namely mechanisms reported by Fukutani et al. (1991), Hennessy et al. (1986), Kara et al. (1988), Miller and Bowman (1989), Puri et al. (1987), Sanogo (1993), Smith et al. (2000), and Warnatz (1981). Of these eight, GRI-Mech 3.0 (Smith et al., 2000) was one of the ones that gave the best agreement with the experiments. In Appendix A, the comparison of CO predictions made by the eight reaction mechanisms is given, as reported in (Musick et al., 1996).

The predictions we make are then compared with experimental data. To this end, an ultra rich combustion test rig was built and operated, and the experimental data are compared with the model predictions. Finally, conclusions based on this work are summarized.

FREELY PROPAGATING FLAME SIMULATIONS

Methane Flammability Limits

Prior to simulating the rich combustion process, the flammability limits of mixtures of CH_4 with different oxidizers have been examined. The effects of temperature and pressure on the upper flammability limit (UFL) of CH_4/O_2 and CH_4/air mixtures were reported by Cooper and Wiezevich (1929) and Vanderstraeten et al. (1997), respectively. Based on the data from these two references, a flammability map was drawn, as shown in Figure 1.

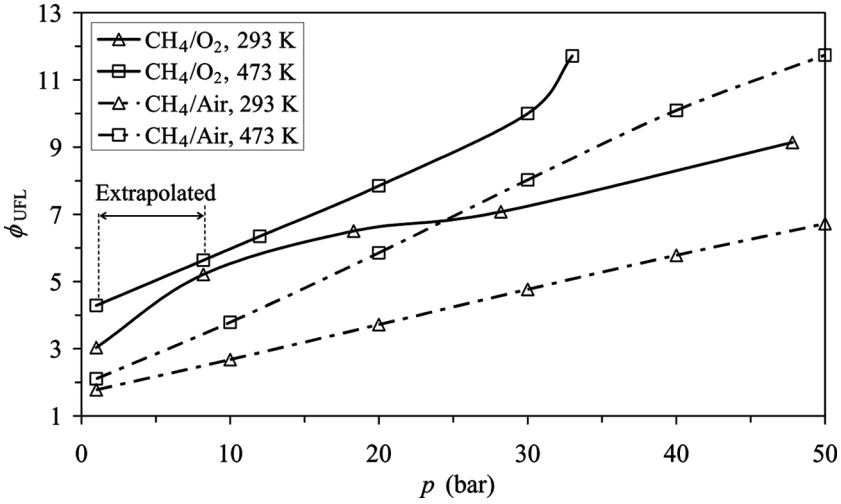

Figure 1 The dependence on pressure of upper flammability limits for CH_4/O_2 and CH_4/air mixtures at inlet temperatures 293 and 473 K (Cooper & Wiezevich, 1929; Vanderstraeten et al., 1997).

In these experimental data, the UFL was expressed as the initial mole fraction of CH_4 in the unburnt mixture. For the present investigation, all flammability data are redrawn to depend on fuel equivalence ratios (calculated on basis of the flammability limits depending on the CH_4 mole fractions). In Figure 1, the resulted equivalence ratios are plotted as a function of pressure for two initial temperatures, 293 K and 473 K, and two types of mixtures, CH_4/O_2 and CH_4/air.

These equivalence ratios are denoted by ϕ_{UFL}. For both types of mixtures, the UFL increases with the pressure and initial temperature. It can be observed in Figure 1 that in CH_4/air mixtures with an initial temperature of 473 K, the ϕ_{UFL} almost triples from a value of 2 at 1 bar to 5.5 at 20 bar.

As expected, for the same initial temperature, CH_4/O_2 mixtures show higher values of the ϕ_{UFL}, which increases from 4.5 at 1 bar (extrapolated value) to 8 at 20 bar. Regarding the NG/NITROX mixtures, the flammability limits are expected to be in between those of CH_4/O_2 and CH_4/air mixtures. The results of freely propagating flames simulations at a pressure of 6 bar and an initial temperature of 673 K are presented later. The values of the ϕ_{UFL} at 6 bar and 473 K are 3 for CH_4/air mixtures and 5 for CH_4/O_2 mixtures. The latter value was approximated by linear extrapolation of the experimental curve. Assuming a further increase of the ϕ_{UFL} when increasing the initial temperature from 473 K to 673 K, it is expected that all mixtures to be investigated, CH_4/O_2, NG/NITROX, and CH_4/air, with equivalence ratios between 1 and 4, pressure of 6 bar, and initial temperature of 673 K, are within the flammability limits.

Freely Propagating Flames

The propagation properties of rich flames, as those obtained by partial oxidation, were studied by simulating freely propagating flames with the code

PREMIX, using the chemical kinetic mechanism from GRI-Mech 3.0 and related thermodynamics and transport files as provided by Smith et al. (2000). The PREMIX code is described in Kee et al. (1985). Three types of mixtures have been simulated: CH_4/O_2, NG/NITROX and CH_4/air. The equivalence ratio was varied from 1 to 4. The equivalence ratio of 1 corresponds to the stoichiometric combustion of CH_4. The equivalence ratio of 4 corresponds to the partial oxidation of CH_4, as described by the chemical reaction in Eq. (1). The pressure and the initial temperature used for the simulations were 6 bar and 673 K.

Figures 2 and 3 present for all flames the simulated laminar flame speed s_L and the adiabatic flame temperature T_{ad}, respectively, as functions of the fuel equivalence ratio ϕ. It can be observed that both s_L and T_{ad} decrease with increasing ϕ for all types of mixtures. The flame speed and temperature also decrease with the increase of the nitrogen content of the oxydizer. Thus, in Figure 2, the flame speed for the$\hat{A}CH_4/O_2$ systems shows values of about 20 to 800 $cm \cdot s^{-1}$, while the CH_4/air systems have a flame speed in the range 5 to 100 $cm \cdot s^{-1}$. NG/NITROX systems are characterized by values of the flame speed in between, in the range 10 to 300 $cm \cdot s^{-1}$. In Figure 3, it can be observed that the flame temperature is in the range 1700–3300 K for CH_4/O_2 mixtures, 1600–2900 K for NG/NITROX mixtures, and 1500–2400 K for CH_4/air mixtures. For comparison, a stoichiometric CH_4/air mixture has a laminar flame speed and an adiabatic flame temperature of about 40 $cm \cdot s^{-1}$ and 2200 K, respectively, at ambient conditions of pressure and initial temperature.

The definition of the calculated adiabatic laminar flame temperature, as presented above in Figure 3, requires some attention, as it is applied in rich flames. In lean one-dimensional flames, the temperature is always observed to rise monotoneously: rising steep at the flame front, followed by an increase of gentle slope downstream, and reaching a maximum value at large but finite distance. The residence

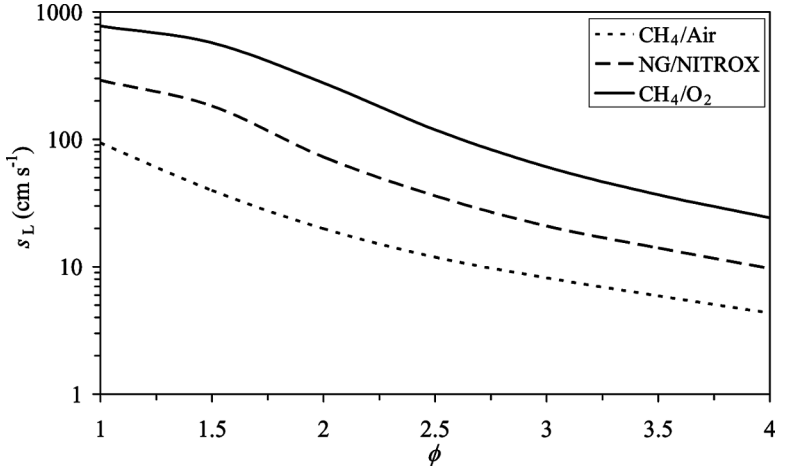

Figure 2 The laminar flame speed (s_L) of rich CH_4/O_2, NG/NITROX and CH_4/air mixtures as a function of equivalence ratio (ϕ). Operating conditions: $p = 6$ bar, $T_{in} = 673$ K. A logarithmic scale was used in the representation.

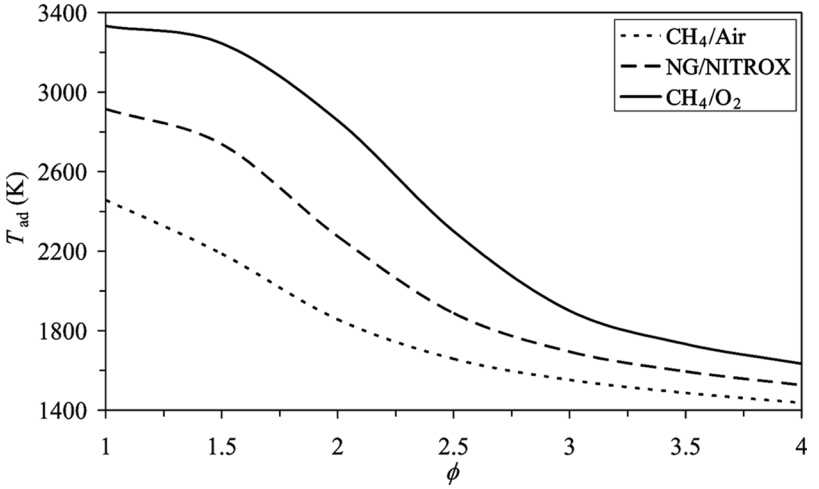

Figure 3 The adiabatic flame temperature (T_{ad}) of the same mixtures and at the same operating conditions as in Figure 2.

time corresponding to the distance downstream the flame front, where the temperature is not changing significantly anymore, is of the order of 50 ms. The end (and maximum) temperature reached at this time scale in a lean adiabatic flame, is almost equal to the equilibrium temperature. In rich flames, however, this is not the case: the maximum temperature, end temperature, and equilibrium temperature are all significantly different. In a rich flame, the temperature rises to a maximum value at the flame front, followed by a decrease downstream, leveling at a very slow rate to an end value. In the present paper, the adiabatic laminar flame speed is defined as the temperature reached in the flame at a large but finite distance from the flame front, where the temperature gradient has become less than the computational accuracy.

Based on the data presented in Figures 2 and 3, the laminar flame speed was plotted on a logarithmic scale against the inverse of the adiabatic flame temperature in Figure 4. This figure shows clearly that the logarithm of the laminar flame speed correlates linearly with the inverse of the adiabatic flame temperature. For that reason, for each type of mixture, it was possible to fit an Arrhenius type function for the laminar flame speed as a function of the adiabatic flame temperature with the calculated points. The general relation between s_L and T_{ad} is approximated by the expression

$$S_L = A_L \, e^{\frac{E_a}{2RT_{ad}}}. \tag{2}$$

In Eq. (2), A_L is a pre-exponential factor of the laminar flame speed, E_a is an activation energy, and R is the universal gas constant. This activation energy corresponds to a global reaction that describes the conversion of reactants to products in the rich combustion process. The dependence of s_L on T_{ad}, in the form of the Arrhenius function given by Eq. (2) is similar to that given by the Zeldovich analysis for the stoichiometric combustion of CH_4 as reported by Warnatz et al. (1996).

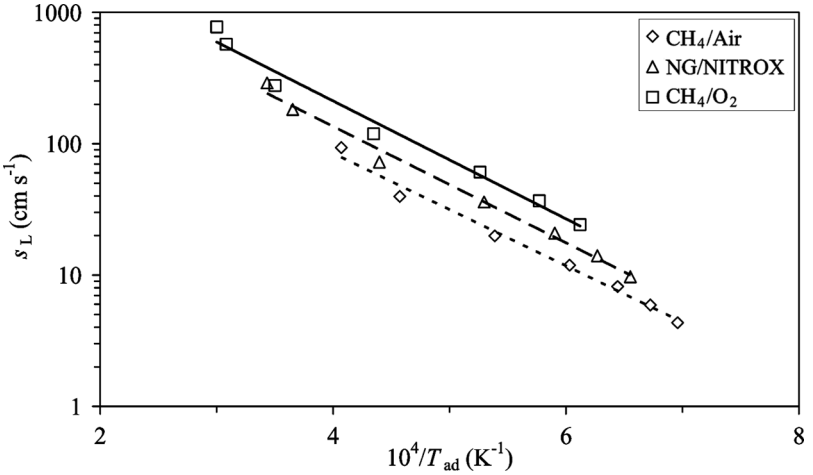

Figure 4 The laminar flame speed as a function of the adiabatic flame temperature for the mixtures represented in Figures 2 and 3, at the same operating conditions.

In that work by Warnatz et al., the adiabatic flame temperature was varied by changing the initial temperature of the mixture, and the equivalence ratio was kept stoichiometric. Warnatz et al. also determined the pressure dependence of the pre-exponential factor. In the present paper, the coefficients of Eq. (2) were fitted for a pressure of 6 bar and an initial temperature of 673 K. The influence of pressure was not investigated. The ratio E_a/R has the unit K and is therefore called the activation temperature, denoted by T_a. The activation temperatures divided by 2 (see Eq. (2)) are given by the slopes of the fitting lines plotted in Figure 4. The rounded values of the pre-exponential factors and the activation temperatures are presented in Table 2. Examining the figures reported in Table 2, it can be noticed that the activation temperatures for all rich mixtures have similar values (around $T_a = 20{,}000$ K: all lines shown in Figure 4 are parallel). Concerning the pre-exponential factors, the lowest value corresponds to the CH_4/air mixtures ($A_L = 4400\,\mathrm{cm \cdot s^{-1}}$), and this value is roughly doubled for NG/NITROX systems and tripled for CH_4/O_2 mixtures. Inspecting the fitting curves in Figure 4, they overlap very well with the calculated points for ultra rich mixtures, characterized by low flame speeds and temperatures ($\phi = 2.5$–4). For less rich mixtures, the accuracy of the correlation with the simulated data decreases with decreasing equivalence ratio. The explanation is the significant change of the chemical kinetics due to the fact that the combustion

Table 2 Activation temperatures and pre-exponential factors for the Arrhenius type laminar flame speed–adiabatic flame temperature correlations

Mixture	T_a (K)	A_L (cm · s^{-1})
CH_4/O_2	20700	13200
NG/NITROX	20400	8000
CH_4/air	19700	4400

of ultra rich mixtures of CH_4 (partial oxidation) produces mainly H_2 and CO, as opposed to the stoichiometric combustion, which leads to the products H_2O and CO_2. The fitting of the data is also less exact for CH_4/O_2 mixtures than for NG/NITROX and CH_4/air mixtures. This is caused by the much larger combustion temperature range spanned by the CH_4/O_2 mixtures compared to the NG/NITROX and CH_4/air mixtures (for the same equivalence ratio interval), and the fact that Eq. (2) is not a fundamental relationship.

To gain insight into the major processes in rich flames, a NG/NITROX freely propagating flame with the equivalence ratio of 3.1 was used for analysis using the PREMIX code. The mole fractions of the main species and the temperature are plotted versus residence time in Figure 5. Residence times were found by integrating the inverse of the predicted gas velocities over the distance traveled in the flame. The flame presents a narrow flame front, with fast oxidizing exothermic reactions, the main products being H_2, H_2O, and CO. Inside this region, all the oxygen is consumed, but unconverted methane will remain to be present in the post flame zone. This post flame zone is characterized by slow endothermic reforming reactions of CH_4 with H_2O. As a result, the H_2O and CH_4 mole fractions decrease, and H_2 and CO mole fractions increase.

In Figure 5, the flame temperature is observed to rise steeply at the flame front due to the exothermic oxydizing reactions to a maximum temperature of about 1800 K. Subsequently, the temperature decreases again in the postflame zone due to the endothermic reforming reactions, to reach an almost constant end temperature of 1680 K at residence time 50 ms. This end temperature is taken here to be the adiabatic flame temperature and can also be read at this value in Figure 3, for equivalence ratio 3.1 in a NG/NITROX system. The adiabatic flame temperature is still higher than the equilibrium temperature, as the reforming reactions have become very slow at the adiabatic flame temperature but are in fact still active. Unfortunately, it would take extremely long residence times to allow the reforming

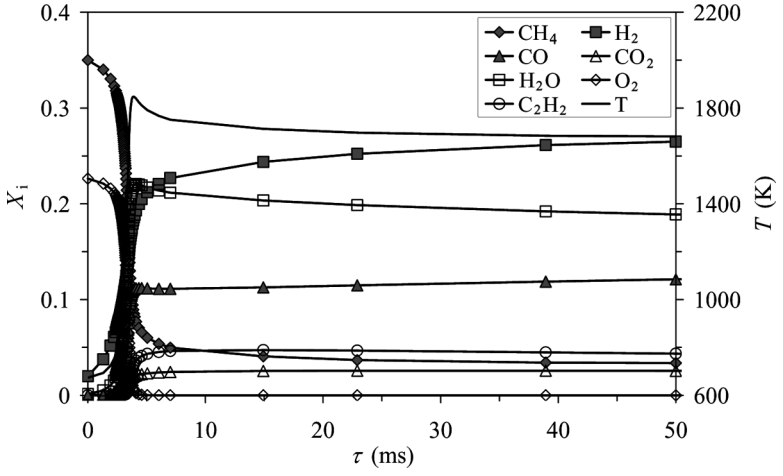

Figure 5 The structure of a rich NG/NITROX flame: temperature and mole fractions of main species as functions of residence time. Operating conditions: $\phi = 3.1$, $p = 6$ bar, $T_{in} = 673$ K.

reactions to reach the equilibrium situation. This is not of any practical use. Hence, in rich flames (similar to lean flames), the end temperature, reached in realistic residence time, can be considered to be the adiabatic flame temperature. However, in contrast to lean flames, in rich flames the adiabatic flame temperature is higher than the equilibrium temperature and lower than the maximum flame temperature. This is caused by the fact that, downstream the flame front, reforming reactions, which are endothermic in character and have very long chemical time scales, are active, and not oxidizing reactions (with an exothermic character), like in lean flames.

The deviation from equilibrium of rich combustion systems as a function of residence time will be discussed for the situation of a perfectly stirred reactor. Here it is calculated that rich combustion systems that exceed a critical equivalence ratio need excessive chemical times to reach equilibrium. A typical time scale for the oxydizing reactions in a laminar flame is 50 ms (see Figure 5). However, in a rich combustion system exceeding the critical equivalence ratio, even 1,000 ms would not suffice to be close to the equilibrium conditions, as will be shown. The critical equivalence ratio for a NG/NITROX system is found to be 2.0, and for a CH_4/O_2 system is 2.5.

Also presented in Figure 5 are the mole fractions of carbon dioxide and acetylene. The carbon dioxide formed in the initial fast reaction zone remains practically constant in the post-flame zone. This shows that the reactions in which CO_2 takes place are too slow to produce any change of its concentration for the residence time investigated (50 ms). As for C_2H_2, this is produced in the initial part of the flame, and then its mole fraction decreases slowly in the post flame zone. The values of the mole fractions of H_2, CO, and C_2H_2 for the flame residence time of 50 ms will be compared with those given by PSR simulations and measurement data. It can be remarked that the post-flame zone of the rich flame discussed here is not in equilibrium, due to the presence of the reforming reactions. This slow approach to equilibrium is very much in contrast with the behavior of lean CH_4 flames.

PERFECTLY STIRRED REACTOR (PSR) SIMULATIONS

PSR Operating Conditions

A number of simulations have been performed with the PSR code from the CHEMKIN package for the rich combustion process. The code is described in Glarborg et al. (1986). Three operating pressures, three residence times, two mixtures, and equivalence ratios between 1 and 4 were investigated. They are shown in Table 3. As far as the pressure is concerned, usually the industrially applied processes run at pressures above 20 bar. The 1 and 6 bar pressures are included here for the study of

Table 3 Case studies for PSR simulations

Mixture	Pressure, p (bar)	Residence time, τ (ms)	Equivalence ratio, ϕ
CH_4/O_2, NG/NITROX, CH_4/air	1, 6, 20	50, 1000, ∞ (equilibrium)	1–4

the pressure effect on the rich combustion process. Regarding the residence time, 50 ms corresponds to the conditions in a practical design, 1000 ms is in the range of residence times reported in the literature dedicated to the partial oxidation process (Mungen & Kratzer, 1951), and an infinite residence time is the limit reached at equilibrium. For each case studied, the equilibrium was determined with the CHEMKIN code EQUIL. In the following sections, the results of the PSR computations are presented.

Equivalence Ratio and Residence Time Effect

Simulations have been performed for the residence times, mixtures, and equivalence ratios presented in Table 3. The pressure was equal to 20 bar for the CH_4/O_2 mixtures and 6 bar for the NG/NITROX mixtures. The initial temperature was 673 K for all simulations, in accordance with data reported in the literature, and the experiments performed.

Based on the calculated molar fluxes of H_2, CO, and C_2H_2, two coefficients of performance, COP_{H_2+CO} and $COP_{C_2H_2}$, were defined as

$$COP_{H_2+CO} = \frac{N^{out}_{H_2} + N^{out}_{CO}}{N^{in}_{CH_4}} \tag{3}$$

$$COP_{C_2H_2} = \frac{N^{out}_{C_2H_2}}{N^{in}_{CH_4}}. \tag{4}$$

In Eqs. (3) and (4), $N^{out}_{H_2}$, N^{out}_{CO}, and $N^{out}_{C_2H_2}$ are the molar fluxes of H_2, CO, and C_2H_2 produced, respectively, and $N^{in}_{CH_4}$ is the molar flux of CH_4 introduced in the reactor. Figures 6 and 7 present COP_{H_2+CO} and $COP_{C_2H_2}$ as functions of the equivalence ratio ϕ, for rich mixtures of NG/NITROX and CH_4/O_2, respectively. As H_2 and CO are the desired products of the rich combustion process, the coefficient of performance COP_{H_2+CO} shows the conversion efficiency of CH_4 to syngas. Considering C_2H_2 as the soot precursor, as in combustion modeling work reported by Lindstedt (1994) and Brookes and Moss (1999), the coefficient of performance $COP_{C_2H_2}$ is a measure for soot formation.

Figure 6 plots the COP's of Eqs. (3) and (4) for NG/NITROX mixtures as a function of ϕ. It can readily be observed that residence time plays a role only for NG/NITROX mixtures with an equivalence ratio higher than 2. For lower equivalence ratios, the rich combustion temperature is sufficiently high to drive the chemical systems to equilibrium in a time shorter than 50 ms. As a result, the values of COP_{H_2+CO} and $COP_{C_2H_2}$, corresponding to the residence times of 50 ms and 1000 ms, overlap the equilibrium values at sufficiently low equivalence ratio. It can be remarked that C_2H_2 is an intermediate species present in the products only under non-equilibrium conditions.

Figure 6 shows that, for equivalence ratios in the range 2–4, COP_{H_2+CO} increases while $COP_{C_2H_2}$ decreases when increasing the residence time from 50 ms to ∞ (equilibrium). Hence, an increase of residence time increases the syngas production and decreases the formation of the soot precursor at given equivalence ratio.

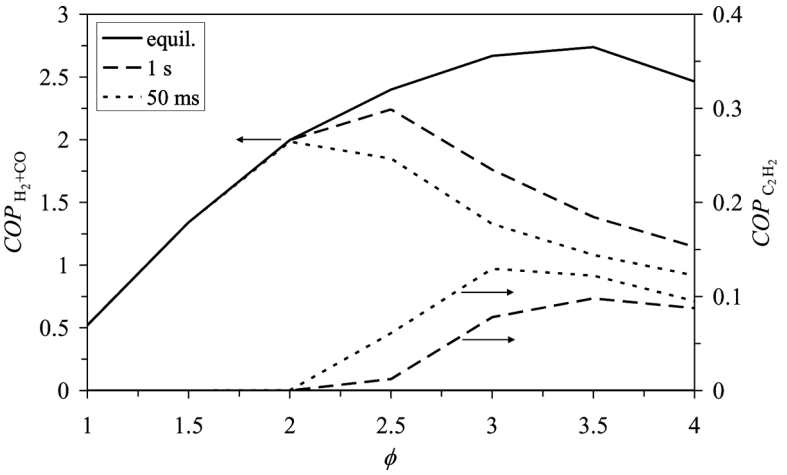

Figure 6 The coefficients of performance COP_{H_2+CO} and $COP_{C_2H_2}$ in NG/NITROX mixtures as functions of equivalence ratio with residence time as a parameter. The type of curve is indicated by the arrows. Operating conditions: $p = 6$ bar, $T_{in} = 673$ K.

With a view to the effect of equivalence ratio, it can be observed in Figure 6 that the calculated COP_{H_2+CO} curves show a maximum value of the coefficient of performance. The maximum value of the COP_{H_2+CO} is about 2 at equivalence ratio 2 and residence time 50 ms. The maximum increases to 2.2 at equivalence ratio 2.5 for at a residence time of 1000 ms. The highest value for the maximum of the COP_{H_2+CO} is reached in the equilibrium situation: 2.6 at equivalence ratio 3.6. For 50 and 1000 ms, the COP_{H_2+CO} decreases to about 1 and in equilibrium to 2.4 at $\phi = 4$.

When the rich combustion of CH_4 would be as described by the global reaction, the maximum value of COP_{H_2+CO} would be 3 and have occurred at an equivalence

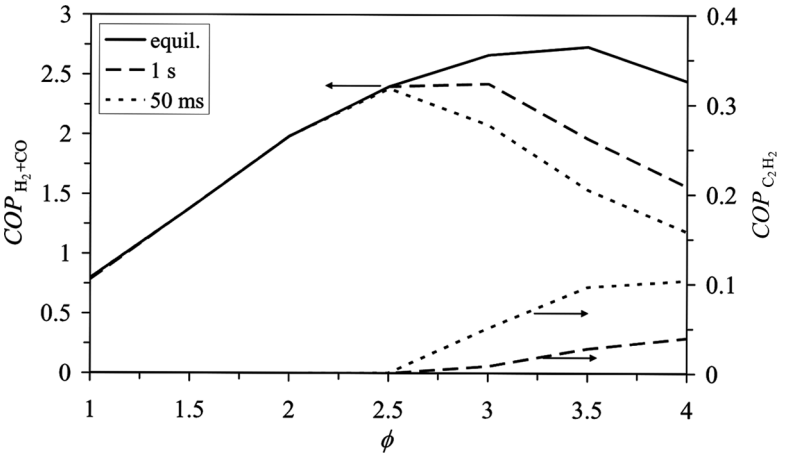

Figure 7 The coefficients of performance COP_{H_2+CO} and $COP_{H_2H_2}$ in CH_4/O_2 mixtures as functions of equivalence ratio with residence time as a parameter. The type of curve is indicated by the arrows. Operating conditions: $p = 20$ bar, $T_{in} = 673$ K.

ratio of 4. This is different from the behavior in Figure 6, even for long residence times. The results displayed in Figure 6 lead to hence two important observations:

1. The equilibrium of the 53 species of the GRI mechanism leads to a lower maximum COP_{H_2+CO} than the one-way reaction of CH_4 and O_2 to CO and H_2, as described by Eq. (1).
2. The maximum value of the COP_{H_2+CO} is not reached at equivalence ratio 4, as expected with only the one way reaction of CH_4 and O_2 to CO and H_2, but at equivalence ratio 3.6.

The answer to the first observation is easily given. The maximum COP_{H_2+CO} equal to 3.0 is reached, according to the definition in Eq. (3), when all CH_4 is converted to CO and H_2. This is a maximum guaranteed not to exceed, and never to be reached when other species like CO_2 and intermediary hydrocarbons are taken into consideration. The answer to the second observation is that at very high equivalence ratio, the chemical system shifts to a situation with higher intermediate species (hydrocarbons) concentrations and a lower temperature. This leads to decreased concentrations of the products CO and H_2, and hence a lower COP.

At finite residence times, the coefficient for the soot precursor increases fast from 0 to about 0.1 when the equivalence ratio exceeds 2. It can be concluded that for maximum syngas output and minimum soot production, the rich combustion reactor should be operated at the equivalence ratio for maximum COP_{H_2+CO}.

Figure 7 plots the COPs of Eqs. (3) and (4) for CH_4/O_2 mixtures as a function of ϕ, with the residence time as a parameter. The behavior is similar to the NG/NITROX systems, but the equivalence ratio from which the residence time has influence on COP_{H_2+CO} and $COP_{C_2H_2}$ is increased from 2 to 2.5. This can be explained by the fact that NG/NITROX mixtures have lower combustion temperatures than CH_4/O_2 mixtures, for the same equivalence ratio, due to the dilution with N_2 (see also Figure 3). It follows that CH_4/O_2 mixtures are in equilibrium for ϕ values of 2–2.5, where the NG/NITROX mixtures are not greater, due to their lower chemical reaction rates. Figure 7 shows that for equivalence ratios in the range 2.5–3 for CH_4/O_2 mixtures, COP_{H_2+CO} increases while $COP_{C_2H_2}$ decreases when increasing the residence time from 50 ms to ∞ (equilibrium). In equilibrium of the CH_4/O_2 mixtures, the $COP_{C_2H_2}$ shows a maximum value of 2.42 at $\phi = 3$ and then decreases to 1.56 at $\phi = 4$. For reasons similar to the NG/NITROX systems, the maximum value in equilibrium of the COP_{H_2+CO} is less than 4, as would be the case if only the species present in Eq. (1) would be taken into account. What is interesting is that the maximum value of the COP_{H_2+CO} in the CH_4/O_2 mixture occurs at a much lower equivalence ratio (3.0 versus 3.6) and that the value itself is lower: 2.4 versus 2.6 as compared to NG/NITROX systems. Apparently, the equilibrium shifts away from CO and H_2 at the much higher equilibrium temperatures achieved in the CH_4/O_2 mixture.

Pressure Effect

In the present section, the effect of pressure in the rich combustion reactor is analyzed. A number of cases have been simulated using the pressures, mixtures,

and equivalence ratios as presented in Table 3. The initial temperature was 673 K and the residence time 50 ms. The two coefficients of performance defined in the previous section (COP_{H_2+CO} and $COP_{C_2H_2}$) have been calculated for the study of the pressure effect on the rich combustion process. In Figure 8, COP_{H_2+CO} in a NG/NITROX mixture is plotted against the equivalence ratio with the pressure as a parameter.

Figure 8 shows a small decrease of the value of COP_{H_2+CO} with pressure for $\phi = 1$–1.5. For the interpretation of this result, it is important to observe that, according to the results presented in Figure 6, the chemical system is in equilibrium at equivalence ratios 1–2. The decrease of the COP_{H_2+CO} can then be explained by Le Chatelier's principle, which states that if a dynamic equilibrium is disturbed by changing the conditions, the position of equilibrium moves to counteract the change. Hence, when the system is described by a global reaction, as given in Eq. (1), the equilibrium will shift to the side of the reaction with fewer molecules, when the pressure is increased. According to reaction 1, this means it shifts away from $CO + 2H_2$; hence, the COP_{H_2+CO} will decrease with increasing pressure.

At equivalence ratios 3–4, the COP_{H_2+CO} increases with pressure. Hence, this behavior is the opposite at equivalence ratios 1–1.5. This can also be explained with Figure 6, which shows that at 50 ms residence times, the system is not in chemical equilbrium at equivalence ratios above 2. For that reason, Le Chatelier's principle cannot be applied. The system is still far from equilibrium and brought closer to it, and it increased COP_{H_2+CO}, due to the increase of reaction rates at increased pressure. In the equivalence ratio range 1.5–3, there is not an effect of pressure, as the effect of the drive toward equilibrium is compensated by the shift of the equilibrium. The results above confirm results reported by Mayland and Hays (1949) and Montgomery et al. (1948).

As far as C_2H_2 is concerned, the value of $COP_{C_2H_2}$ is 0 under equilibrium conditions (according to Figure 6, this is the range $\phi = 1$–2). The value of $COP_{C_2H_2}$

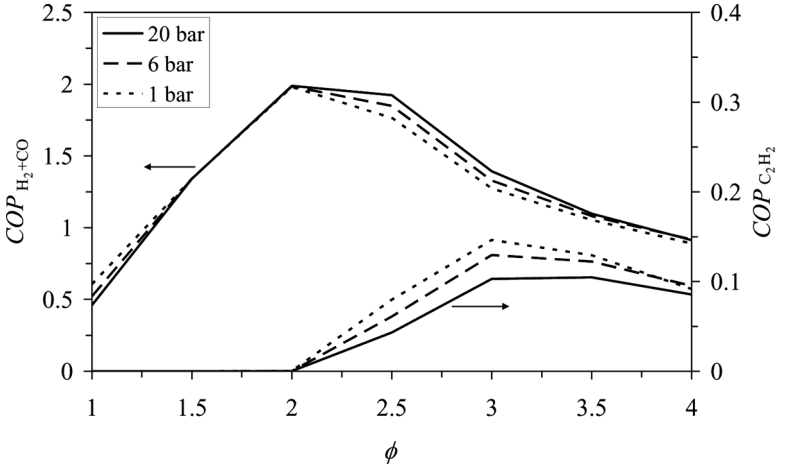

Figure 8 The coefficients of performance COP_{H_2+CO} and $COP_{C_2H_2}$ in NG/NITROX mixtures as functions of equivalence ratio at $\tau = 50$ ms with pressure as a parameter. Initial temperature 673 K.

decreases when increasing the pressure in the non-equilibrium region ($\phi = 2$–4). Given that C_2H_2 is considered the soot precursor, the latter result indicates that more soot is likely to form at lower pressures and equivalence ratios over 2. This is in accordance with Christensen and Primdahl (1994), where it is stated that in autothermal reforming (ATR), low pressures (<12 bar) have to be avoided because of soot formation. However, many other references report an increase of the soot volume fraction f_S with pressure p following the relation

$$f_S \approx p^m. \tag{5}$$

In Eq. (5), $1 \leq m \leq 2$ for laminar rich premixed C_2H_4/air flames and various laminar and turbulent diffusion flames (Fischer & Moss, 1998) and $m = 3$ for laminar CH_4/air non-premixed flame at pressures lower than 30 bar (Roditcheva & Bai, 2001). The opposite reported dependence of soot formation on pressure may be caused by two factors. First, the dependence of soot formation on C_2H_2 is via the complex and not completely mapped processes of nucleation and surface growth (Bockhorn, 1994). Second, the soot formation is probably significantly influenced by the operating conditions and the equivalence ratio, which are different in Christensen and Primdahl (1994) from Fischer and Moss (1998) and Roditcheva and Bai (2001).

Summarizing the above, it can be concluded that for non-equilibrium conditions ($\phi = 2$–4) in the rich combustion process, the production of CO and H_2 increases with pressure. As for C_2H_2, considered the soot precursor, it was calculated that the production of C_2H_2 in non-equilibrium conditions decreases with increasing pressure.

Similar results on the effect of pressure, as shown in Figure 8 for NG/NITROX mixtures, have been obtained for CH_4/O_2 mixtures.

EXPERIMENTAL VALIDATION BY A NATURAL GAS ULTRA RICH COMBUSTION EXPERIMENT

Test Rig Setup

In order to demonstrate the production of syngas on basis of natural gas and NITROX (air enriched to 40 vol % oxygen) by ultra rich combustion, and to compare the model predictions for the PSR with practical data, a test rig was built and operated at the University of Twente. The layout is depicted in Figure 9. Natural gas is supplied to the test rig by a 10 bar compressor fed by the gas network. The composition of the natural gas is specified in Table 4. The natural gas flow is mixed in the mixer manifold with an air flow delivered by a 10 bar air compressor and an oxygen flow delivered by a set of bottles. All mass flows are individually set by mass flow controller valves. The mix of air, oxygen, and natural gas is heated subsequently to 673 K in a shell and tube heat exchanger by a 703 K air flow. The hot mix of reactants is fed to the reactor. The reactor geometry is sketched in Figure 10. The premixed preheated natural gas/air/oxygen flows through a perforated plate to a radial slot swirler. The swirled gas enters at high velocity (to prevent flame flash back) through an annular passage, the cylindrical reactor chamber, with a diameter of 100 mm and length of 500 mm. Due to the expansion in diameter, the swirled gas

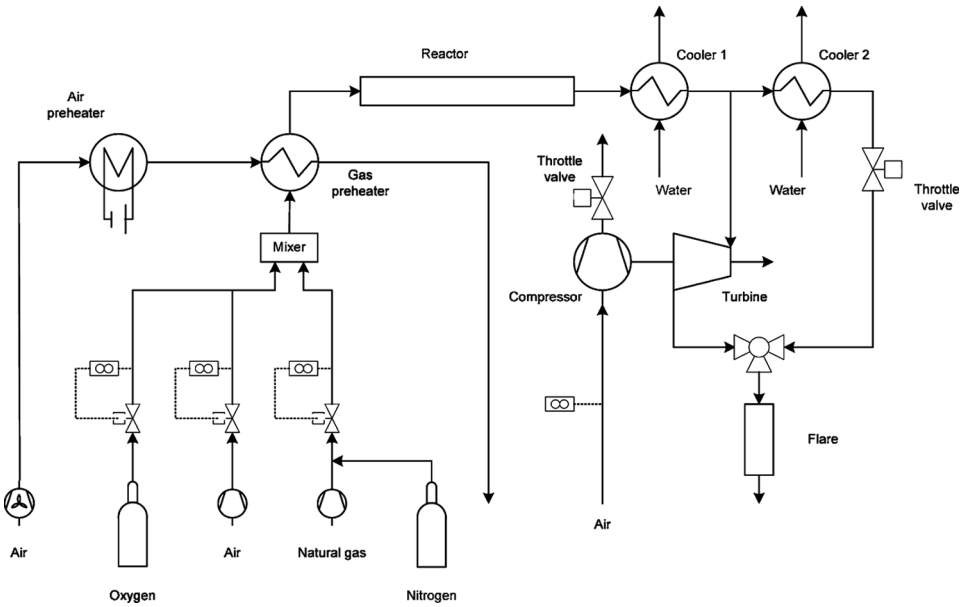

Figure 9 Test rig lay out for partial oxidation of preheated natural gas/NITROX mixtures to syngas.

is swept to large radius and induces a central recirculation area at the axis. This hot recirculating flow stabilizes the ignition of the reactants. At startup, the recirculating flow is ignited by a spark plug located at the burner mouth. The reactor has ceramic lined walls with very low heat loss. The nominal average residence time has an approximate value of 50 ms. At the exit of the reactor, the extremely hot syngas flow is cooled in a shell and tube heat exchanger by a water flow to an intermediate temperature of 1023 K. At this point, two process paths were possible. In cases relevant for data presented in this paper, the syngas flow was cooled further down to 313 K by a second shell and tube heat exchanger by a water flow. Subsequently, the syngas flow is throttled in a valve to atmospheric pressure and discharged safely into the atmosphere by combustion in a flare. Hence, the reactor pressure is controlled by the throttle valve.

Table 4 Composition of Groningen natural gas

Species	[% vol.]
CH_4	81.30
C_2H_6	2.85
C_3H_8	0.37
C_4H_{10}	0.14
C_5H_{12}	0.04
C_6H_{14}	0.05
N_2	14.35
O_2	0.01
CO_2	0.89

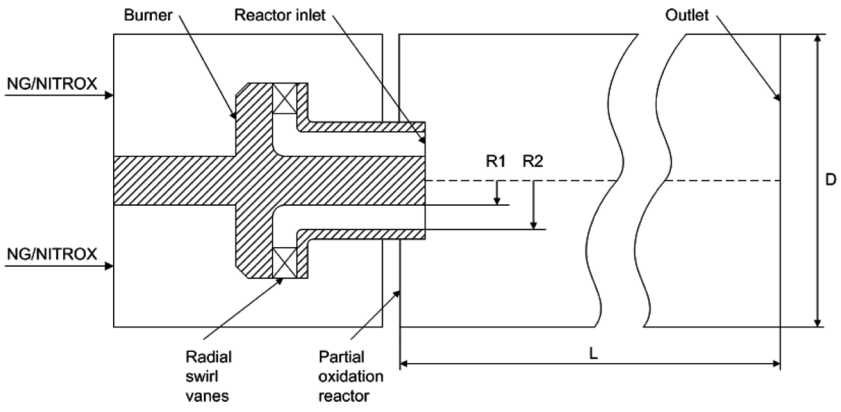

Figure 10 Design of the partial oxidation reactor.

For demonstration purposes not relevant here, the 1023 K syngas flow could also by routed to the flare by passing a small turbine expander. It was demonstrated that the turbine delivered a power to the load compressor of about 5 kW at turbine pressure ratio 2, syngas flow 300 kW, and syngas reactor pressure 3 bar.

The static reactor pressure (with a pressure transducer) and the reactor inlet temperature were continuously measured with a thermocouple. Online gas samples were taken of the cooled down product gas just downstream of the throttle valve. To prevent the condensation of water, the sample is transported with a heated hose to the analysis equipment. Before it is analyzed, the gas sample is cooled to 273 K to remove the water vapor. All measurements are therefore dry measurements, and in comparison to the simulation results are post-processed accordingly.

The accuracy of the measurements is influenced by several aspects of the measuring system. The gas sample was cooled rapidly to a temperature where the reactions are frozen in time. The analyzers were calibrated before and after the session. The differences between these calibrations were less than 1% of the calibration value. For that reason, it can be assumed that the measured value is close to the actual concentration in the gas sample.

Most product gas composition measurements were done with the online equipment while exploring the effect of equivalence ratio. More detailed measurements were performed at the nominal operating point of the reactor. The product gas composition measurement at the nominal operating point of the reactor (300 kW/3 bar) was done batch-wise with a gas chromatograph. This latter instrument allowed the measurement of not only CO, but also H_2 and C_2H_2. The gas analysis equipment is specified in Table 5.

Test Rig Operation Conditions and Ignition Procedure

The production of syngas requires carefully prepared operating procedures and safety measures. The test rig was placed in a laboratory with explosion-safe construction and equipped with a hydrogen, carbon monoxide, and unburnt hydrocarbons

Table 5 Gas concentration measurement equipment

Species	Analyzer	Range	Calibration
CO	Beckman Industrial model 870	0–31.4 vol%	29.7 vol%
CO_2	Maihak Multor 610	0–25 vol%	14.76 vol%
H_2, CO, CH_4, CO_2, C_2H_2	Varian Star 3400 CX	0–40 vol%	Species-dependent

detection system. The entire setup was used by remote control from a control room. The test rig could not be started on the very well premixed natural gas/air mixture. It appeared that the flame flashed back from the reactor through the preheated mixture into the hot gas preheater at the moment of ignition, despite the flame arrestors that were built in the burner inlet passage. For that reason, the design was adapted and the reactor was equipped with a startup gas injector at the burner inlet. This provided a partially premixed gas flow to the reactor. This flow was ignited by the spark plug and without flash back. After the partially premixed flow was ignited and a flame was stabilized at the burner exit in the reactor, the natural gas flow was switched to the mixer and passed the gas preheater. From that moment, the reactor was operated on a well premixed and preheated natural gas/NITROX mixture.

The reactor was started by the following procedure. First, the reactor was warmed to 573 K by running hot air via the preheater into the reactor at 673 K for an hour. During this time, the mass flow controller valves for natural gas and oxygen remained closed. Subsequently, the natural gas valve to the startup gas injector was opened at 30 kW and a stoichiometric fuel/air ratio. With the spark plug, the partially premixed natural gas/air flow was then ignited. Some time was allowed in this stoichiometric combustion operation to heat up the reactor to about 1300 K. Subsequently, the natural gas valve to the mixer was opened, and the natural gas valve to the startup injector was closed gradually. Hence, the natural gas flow was then routed through the mixer, preheated, and increased in power to 100 kW at pressure 1 bar. The air flow was adapted to the equivalence ratio of 2 or more, while the oxygen flow was set to reach an oxidizer composition of 40%.

Comparison of Measured and Predicted Product Gas Composition

With the test rig and procedure described above, the composition of the syngas produced was measured as a function of equivalence ratio. The CO concentration was determined online with the use of the sample probe. The reactor residence time was in all measurements approximately 50 ms, at a natural gas flow equivalent to a power of 100 kW and a pressure of 1 bar. This is with the exception of the point with highest equivalence ratio, which was taken at a natural gas flow equivalent to 300 kW and a pressure of 3 bar. The oxidizer was NITROX (air enriched with oxygen to a concentration of 40%). The results are depicted in Figure 11. The CO concentration in the syngas is low at low equivalence ratio (12% at equivalence ratio 1.3). With increasing equivalence ratio, the CO concentration increases to a maximum of 22% at equivalence ratio 2.0. In chemical equilibrium and hence very large residence times, the CO concentration would continue to rise with the equivalence ratio. This is predicted by the simulation model in Figure 6. It can be observed

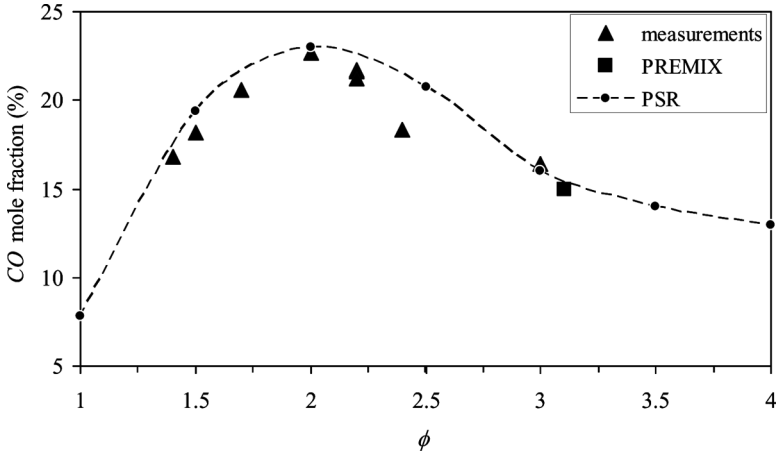

Figure 11 Comparison of measured and predicted CO concentration in syngas produced on basis of natural gas/NITROX.

in Figure 10 that at a residence time of 50 ms, this is not the case. With increasing equivalence ratio, the CO concentration is decreasing again to a value of 16% at equivalence ratio 3. These measured data are compared to the results obtained by the model for a PSR with residence time of 50 ms. They are plotted together with data for a PSR with a simulated residence time of 50 ms for comparison in Figure 11. The measured CO concentration of the syngas compares very well with the CO concentration as calculated in the PSR. It is very important to note that in the measurements, the maximum CO concentration reached is 22%, and that it occurs at equivalence ratio 2. This compares very well to the maximum value and equivalence ratio as calculated by the model for the PSR. This indicates that the chemical reaction kinetics in a stirred reactor give a good estimate of the processes in the reactor in the test rig.

More detailed gas composition measurements were performed at the nominal point of operation at a natural gas flow equivalent to a power of 300 kW and pressure 3 bar. With the use of the gas chromatograph, offline samples were analyzed on concentration of H_2, CO, CO_2, and C_2H_2. The latter species is important as a precursor of soot formation. Table 6 gives the measured concentrations of these species and their values as calculated by the model at 50 ms residence time in the stirred reactor and in the premixed laminar flame and the equilibrium situation. The important conclusion can be drawn that the measured data for H_2 and CO compare very well with the data in the stirred reactor computation. They are for these species approximately 30% and 16%, respectively. The syngas production as measured in the turbulent reactor and predicted in the stirred reactor is of similar value as predicted in the laminar flame (see Table 6 for dry results). Here, the rounded H_2 and CO concentrations were 33% and 15% at 50 ms residence time. The equilibrium concentrations are higher by a factor 1.5 as measured for syngas in the turbulent reactor. Hence, similar to the PSR calculations, the measured syngas yield is decreased.

Table 6 Measured and predicted concentrations of CO, H_2, and C_2H_2 in produced syngas

Species concentration [vol %]	H_2	CO	CH_4	CO_2	C_2H_2
Measured in test rig	30.6	16.4	5.0	3.6	7.0
PSR: predicted at 50 ms	29.7	16.0	5.6	3.3	4.5
PREMIX: predicted at 50 ms	32.7	14.9	4.2	3.2	5.4
Chemical equilibrium	44.3	24.1	0	1.5	0

The predictions given are on basis of 50 ms residence time in a stirred reactor (CHEMKIN PSR code) and on basis of the 50 ms residence time in a premixed laminar flame (CHEMKIN PREMIX code). All predicted values have been recalculated as dry mole fractions in order to be comparable with the measured ones. Operating conditions for predictions: p = 6 bar, fuel equiv. ratio = 3 for PSR and EQUIL and 3.1 for PREMIX.

An important reason for the decreased yield of syngas is the residual amount of CH_4. In equilibrium, all CH_4 is converted to syngas, while both the measurements and the model predictions at 50 ms show a residual CH_4 concentration of 5%. Another explanation for the decreased yield of syngas is the conversion of CH_4 to C_2H_2. This species is absent in equilibrium but both in the measurements and in the model predictions at 50 ms observed at concentrations of 5–7%. Not only will this be at the cost of syngas production, but it will also lead to the formation of soot. This process is evaluated and predicted with the use of CFD in Albrecht and Kok (2009).

The effect of pressure is predicted to be small, even when increasing the pressure from 1 to 20 bars. The measured operational point at 3 bar compares very well in trend with the other measured points at 1 bar and 50 ms in Figure 11. For these reasons, a systematic investigation of the effect of pressure was not pursued in the measurements. One important aspect of pressure was observed, however, and this was the effect on flammability. At equivalence ratios above 2.2, the reactor extinguished at pressure 1 bar and power 100 kW (residence time 50 ms). For that reason, the measurement point in Figure 11 at equivalence ratio 3 had to be observed at pressure 3 bar (300 kW), where stable operation proved to be possible. This is in line with the flammability limits and their pressure dependence, as outlined in Figure 1.

CONCLUSIONS

The process of very rich combustion of natural gas has been simulated in freely propagating flames and perfectly stirred reactors. Different types of mixtures and operating conditions have been investigated numerically. The predicted results have been compared to measurements in an ultra rich combustor test rig. The results of the simulations, the experiments, and their comparison can be summarized as follows.

All types of investigated mixtures (CH_4/O_2, NG/NITROX, and CH_4/air) with equivalence ratios between 1 and 4 are between the flammability limits at pressures greater than or equal to 6 bar and an initial temperature of 673 K. At atmospheric pressure, the flammability limits the equivalence ratio to approximately 2. This equivalence ratio limit increases with pressure. The flammability observed in the experiments at 1 and 3 bars was in line with the flammability limits described above.

Ultra rich NG/NITROX mixtures at a pressure of 6 bar and with an initial temperature of 673 K have computed laminar flame speeds in the range 10–300 $cm \cdot s^{-1}$. In a rich flame, the adiabatic flame speed (when taken to be the flame end temperature) is lower than the maximum flame temperature, but higher than the equilibrium temperature. For all rich mixtures investigated, the laminar flame speed is a function of the adiabatic flame temperature following an Arrhenius type expression. The activation temperature is about 20,000 K and has a minor dependence on the type of the mixture. As opposed to the activation temperature, the pre-exponential coefficient is a strong function of the type of the mixture. The expressions found are best fitted to ultra rich mixtures, with equivalence ratios in the range 2.5–4.

The post-flame zone of ultra rich flames is dominated by slow endothermic reforming reactions of CH_4 with H_2O. This is in contrast with lean or stoichiometric flames, for which the post flame zone is in equilibrium. The slow endothermic reforming reactions determine the time necessary to reach chemical equilibrium and the ultimate conversion of CH_4. The time necessary to reach equilibrium increases with equivalence ratio.

The PSR calculations show that, for NG/NITROX mixtures with equivalence ratios from 1 to 2 and CH_4/O_2 mixtures with equivalence ratios in the range 1–2.5, the products of the CH_4 combustion/partial oxidation are in chemical equilibrium. The CH_4/O_2 mixtures are in equilibrium at larger equivalence ratios than NG/NITROX mixtures due to their higher combustion temperatures and hence higher chemical reaction rates. The location of the equilibrium is dependent on pressure. When the pressure is increased, the equilibrium shifts to CH_4, in line with Le Chatelier's principle. This leads to a decrease in CH_4 conversion to CO and H_2. Hence, at equivalence ratios between 1–2, an increased pressure leads to reduced methane conversion.

For ultra rich mixtures (equivalence ratio of 2–4 for NG/NITROX and 2.5–4 for CH_4/O_2), the residence time necessary for the rich combustion process to reach equilibrium is very long, in excess of 1,000 ms. When the chemical equilibrium conditions are reached, a maximum conversion of CH_4 to H_2 and CO is achieved at equivalence ratio 3.5 at a value of 2.6 for COP_{H_2+CO} in NG/NITROX mixtures. In mixtures, the maximum value is reached at equivalence ratio 3.0 and value 2.4 for the COP_{H_2+CO}. This is less than for NG/NITROX systems because the equilibrium has shifted due to the elevated temperatures in CH_4/O_2 mixtures.

For more practical situations, the residence times will be of the order of 50 ms, and the chemical system will be far from equilibrium. Hence, the conversion of CH_4 to H_2 and CO is far from the maximum as possible in the equilibrium. In this situation, increasing the pressure will lead to a move toward equilibrium and hence an increase of the conversion of CH_4 to H_2 and CO. Thus, where for moderately rich mixtures an increase of pressure will decrease the methane conversion, for very rich mixtures it will increase the methane to syngas conversion.

When the rich combustion process is in equilibrium, C_2H_2 (considered a major soot precursor) is not present in significant concentrations in the product gas mixture. This is the case for low equivalence ratios, below 2, or exceptionally long residence times. In other conditions, C_2H_2 is present in the gas produced by the rich combustion process. When the pressure is increased, the system kinetics

becomes faster, and the system comes closer to equilibrium. Therefore, an increase of pressure will lead to decreased C_2H_2 concentrations, and probably less soot formation

Finally, an increase of pressure can be observed to lead to increased flammability of the rich gas mixture.

In the test rig, measurements of CO concentration as a function of equivalence ratio were performed at residence time 50 ms. These measurements compare very well with data computed for the product gas of a perfectly stirred reactor with identical residence time. A maximum CO concentration at equivalence ratio 2 was found in both measurements and PSR calculations. At 300 kW/3 bar measurements were performed of concentrations of H_2, CO, CH_4, and C_2H_2. The measured gas concentrations compared very well with the calculations by the model for the perfectly stirred reactor.

NOMENCLATURE

Acronyms

COP	coefficient of performance
DME	di-methyl-ether
NG	natural gas
NITROX	mixture of nitrogen and oxygen
PSR	perfectly stirred reactor
UFL	upper flammability limit

Latin

A_L	pre-exponential factor of laminar flame speed, $cm \cdot s^{-1}$
CH_4	methane
C_2H_2	acetylene
C_2H_4	ethylene
CO	carbon monoxide
CO_2	carbon dioxide
E_a	activation energy, $kJ\,kmol^{-1}$
f_S	soot volume fraction
H_2	hydrogen
H_2O	water
Δh	heat of reaction, $kJ\,mol^{-1}$
N_2	nitrogen
N_i	moles of species i, kmol
O_2	oxygen
p	pressure, bar
R	universal gas constant, $kJ\,kmol^{-1}\,K^{-1}$
s_L	laminar flame speed, $cm\,s^{-1}$
T	temperature, K
T_a	activation temperature, K
T_{ad}	adiabatic flame temperature, K
X_i	mole fraction of species i

Greek Symbols

ϕ	fuel equivalence ratio
ϕ_{UFL}	upper flammability limit equivalence ratio
τ	residence time, ms

Subscripts and Superscripts

i	species index
in	inlet or initial conditions
m	pressure exponent
out	outlet

REFERENCES

Albrecht, B.A. 2004. Reactor modeling and process analysis for partial oxidation of natural gas, Ph.D. thesis, University of Twente, Enschede, The Netherlands.

Albrecht, B.A. and Kok, J.B.W. 2009. Reaction progress variable modeling of premixed, swirl stabilized, turbulent rich combustion, in preparation.

Albrecht, B.A., Kok, J.B.W., and van der Meer, Th.H. 2007. Co-production of synthesis gas and power by integration of partial oxidation reactor, gas turbine and air separation unit. *Int. J. Exergy*, **4**, 357.

Bockhorn, H. (Ed.). 1994. *Soot formation in combustion—mechanisms and models*, Springer-Verlag, Berlin–Heidelberg–New York.

Bowman, C.T., Frenklach, M., Gardiner, B., Smith, G., and Serauskas, B. 2001. *GRI-Mech 3.0*, Gas Research Institute, Chicago, Illinois, USA. Available at: http://www.me.berkeley.edu/gri-mech/index.html (accessed 2003).

Brookes, S.J. and Moss, J.B. 1999. Predictions of soot and thermal radiation properties in confined turbulent jet diffusion flames. *Combustion and Flame*, **116**, 486.

Burgt, M.J. van, and Leeuwen, C.J. van. 1988. The shell middle distillate synthesis process. In Biddy, D.M., Chang, C.D., Howe, R.F., and Yurchak, S. (Eds.). *Methane Conversion*, Elsevier Publishers B.V., Amsterdam, 473.

Christensen, T.S. and Primdahl, I.I. 1994. Improve syngas production using autothermal reforming. *Hydrocarbon Processing*, March, 39.

Cooper, C.M. and Wiezevich, P.J. 1929. Effects of temperature and pressure on the upper explosive limit of methane-oxygen mixtures. *Industrial and Engineering Chemistry*, **21**, 1210.

Fischer, B.A. and Moss, J.B. 1998. The influence of pressure on soot production and radiation in turbulent kerosene spray flames. *Combust. Sci. and Tech.*, **138**, 43.

Fukutani, S., Sakaguchi, K., Kunioshi, N., and Jinno, H. 1991. Combustion reactions in methane-air premixed flames. *Bull. Soc. Chim. Japan*, **64**, 1623.

Geerssen, T.M. 1988. *Physical Properties of Natural Gases*, N.V. Nederlandse Gasunie. Groningen, The Netherlands.

Glarborg, P., Kee, R.J., Grcar, J.F., and Miller, J.A. 1986. PSR: A Fortran program for modeling well-stirred reactors. Technical Report SAND86-8209, Sandia National Laboratories, Albuquerque, New Mexico, and Livermore, California, USA.

Hennessy, R.J., Robinson, C., and Smith, D.B. 1986. A comparative study of methane and ethane flame chemistry by experiment and detailed modelling. *21st Symposium (International) on Combustion*, The Combustion Institute, 761.

Kara, S.B., Gutman, D., and Senkan, M. 1988. Chemical kinetic modeling of fuel-rich $CH_3Cl/CH_4/O_2/Ar$ flames. *Combust. Sci. Tech.*, **60**, 45.

Kee, R.J., Grcar, J.F., Smooke, M.D., and Miller, J.A. 1985. A Fortran program for modeling steady laminar one-dimensional premixed flames. Technical Report SAND85-8240, Sandia National Laboratories, Albuquerque, New Mexico, and Livermore, California, USA.

Kee, R.J., Rupley, F.M., and Miller, J.A. 1989. CHEMKIN-II: A Fortran chemical package for the analysis of gas-phase chemical kinetics. Technical report SAND89-8009, Sandia National Laboratories, Albuquerque, New Mexico, and Livermore, California, USA.

Lindstedt, P.R. 1994. Simplified soot nucleation and surface growth steps for non-premixed flames. In Bockhorn, H. (Ed.) *Soot Formation in Combustion—Mechanisms and Models*, Springer-Verlag, Berlin–Heidelberg–New York, 417.

Mayland, B.J. and Hays, G.E. 1949. Thermodynamic study of synthesis gas production from methane. *Chemical Engineering Progress*, **45**, 452.

Miller, J.A. and Bowman, C.T. 1989. Mechanism and modeling of nitrogen chemistry in combustion. *Progress Energy Combustion Sciences*, **15**, 287.

Montgomery, C.W., Weinberger, E.B., and Hoffman, D.S. 1948. Thermodynamics and stoichiometry of synthesis gas production. *Industrial and Engineering Chemistry*, **40**, 601.

Mungen, R. and Kratzer, M.B. 1951. Partial combustion of methane with oxygen. *Industrial and Engineering Chemistry*, **43**, 2782.

Musick, M., van Tiggelen, P.J., and Vandooren, J. 1996. Detailed mechanism of $CH_4/O_2/Ar$ flames and modeling in fuel-rich conditions. *Bull. Soc. Chim. Belg.*, **105**, 555.

Puri, I.K., Seshadri, K., and Smooke, M.D. 1987. A comparison between numerical calculations and experimental measurements of the structure of a counterflow methane-air diffusion flame. *Combust. Sci. Tech.*, **56**, 1.

Roditcheva, O.V. and Bai, X.S. 2001. Pressure effect on soot formation in turbulent diffusion flames. *Chemosphere*, **42**, 811.

Sanogo, O. 1993. Etude experimentale et modelization de la structure de flammes: Applications a la recherche de substitute de halons. PhD Thesis, University of Orleans.

Smith, G.P., Golden, D.M., Frenklach, M., Moriarty, N.W., Eiteneer, B., Goldenberg, M., Bowman, C.T., Hanson, R.K., Song, S., Gardiner, W.C., Jr., Lissianski, V.V., and Qu, Z. 2000. GRI 3.0 Mech. Available at: http://www.me.berkeley.edu/gri_mech/ (accessed 2001).

Vanderstraeten, B., Tuerlinckx, D., Berghmans, J., Vliegen, S., Van't Oost, E., and Smit, B. 1997. Experimental study of the pressure and temperature dependence on the upper flammability limit of methane/air mixtures. *Journal of Hazardous Materials*, **56**, 237.

Warnatz, J. 1981. The structure of laminar alkane-, alkene-, and acetylene flames. *18th Symposium (International) on Combustion*, The Combustion Institute, 369.

Warnatz, J., Maas, U., and Dibble, R.W. 1996. *Combustion: Physical and Chemical Fundamentals, Modeling and Simulation, Experiments, Pollutant Formation*, Springer, Berlin, 118.

APPENDIX A: APPLICABILITY OF GRI-MECH REACTION MECHANISM FOR RICH COMBUSTION

In Musick et al. (1996), laminar premixed $CH_4/O_2/Ar$ flames at equivalence ratios between 0.92 and 1.94 and low pressures (20–60 Torr) have been simulated using the PREMIX code with eight reaction mechanisms. The performance of these mechanisms in predicting CO is shown in Figure A1. It can be noticed that GRI-Mech gives one of the best predictions of CO mole fractions. Other well-performing mechanisms are ML and SENK. The comparison presented in Figure A1 corresponds to a $CH_4/O_2/Ar$ flame with the fuel equivalence ratio $\phi = 1.68$ ($X_{CH_4} = 0.235$, $X_{O_2} = 0.279$, $X_{Ar} = 0.485$) at a pressure $p = 40$ Torr and at an initial temperature $T = 530$ K.

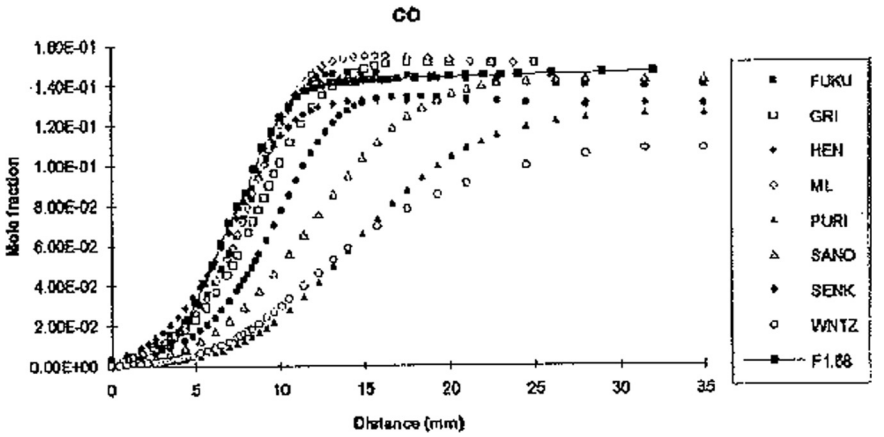

Appendix 1 Experimental (symbol-line) and calculated (symbols) mole fraction profiles of CO in a premixed $CH_4/O_2/Ar$ rich flame with $\phi = 1.68$. Abbreviations: FUKU = Fukutani, 1991; GRI = Smith et al., 2000; HEN = Hennessy et al., 1986; ML = Miller and Bowman, 1989; PURI = Puri et al., 1987; SANO = Sanogo, 1993; SENK = Kara et al., 1988; WRNT = Warnatz, J., 1981. [Reproduced from Musick et al., 1996.]